Archives of Materials Science and Engineering

Volume 101
Issue 1
January 2020
Pages 5-14

International Scientific Journal
published monthly by the
World Academy of Materials
and Manufacturing Engineering

DOI: 10.5604/01.3001.0013.9501

A new ceramic composite based on spherical aluminium oxide for auxiliary panels in high-temperature firing processes

M. Spyrka, R. Atraszkiewicz, L. Klimek *
Institute of Materials Engineering, Lodz University of Technology,
ul. Stefanowskiego 1/15, 90-924 Łódź, Poland
* Corresponding e-mail address: leszek.klimek@p.lodz.pl
ORCID identifier: https://orcid.org/0000-0003-3617-8225 (L.K.)

ABSTRACT

Purpose: The subject of the research and investigation is a new ceramic foundry composite based on a spherical form of aluminium oxide. It is intended to limit the occurrence of technological problems related to the appropriate selection of auxiliary refractory materials, such as cracking, high heat capacity and variable coefficient of thermal expansion.

Design/methodology/approach: A composite ceramic material with the spherical form of aluminium oxide included allows to reduce mass and stabilize characteristics of dimensional changes as a function of temperature in auxiliary panels in high-temperature firing processes with typical manufacturing process of the ceramics, which is gravity casting, drying and high-temperature firing.

Findings: The study showed that the quantitative share of the spherical form of Al_2O_3 in the volume of ceramic material has a major impact on its properties. An increased share of spheres translates into greater material porosity and lower matrix density but also, by reducing the cross-section, into decreased strength properties. In the case of the developed ceramic material, there is no visible trend of a decrease in the coefficient of thermal expansion with increasing temperature, which is the case with traditional ceramic materials.

Research limitations/implications: The strength of presented composite isn't good and constitutes a further direction of research and development of the material.

Practical implications: Although decreased strength properties, the composite with no visible trend of a decrease in the coefficient of thermal expansion with increasing temperature could be used as panels in high-temperature firing processes.

Originality/value: New ceramic foundry composite based on a spherical form of aluminium oxide for auxiliary panels in high temperature processes.

Keywords: Ceramics, Mechanical properties, Holospheres, Al_2O_3

Reference to this paper should be given in the following way:

M. Spyrka, R. Atraszkiewicz, L. Klimek, A new ceramic composite based on spherical aluminium oxide for auxiliary panels in high-temperature firing processes, Archives of Materials Science and Engineering 101/1 (2020) 5-14. DOI: https://doi.org/10.5604/01.3001.0013.9501

MATERIALS

1. Introduction

The manufacturing of ceramic products is inseparably connected with high-temperature firing processes. Regardless of the final product's intended use, temperature plays a key role in influencing mechanical, physical and functional properties. Along with technical progress, the need to search for new ceramic materials characterised by increased fire resistance compared to conventionally used ceramics increased.

One of the challenges is the proper selection of auxiliary elements during the firing process e.g. such as refractory panels. In the ceramics industry, the widely known ceramics based on mullite, silicon carbide or aluminium oxide are used for various auxiliary elements such as shelves, trays and cassettes needed to carry out high-temperature firing processes.

Mullite ceramics are widely used because of the low thermal conductivity, moderate thermal stability and thermal expansion, excellent resistance to thermal shock, good chemical resistance and high-temperature stability as well as mechanical properties [1-6]. The thermo-mechanical properties of mullite-based ceramics directly depend on the glassy phase present in them. The glassy phase has a positive effect on the material's resistance to thermal shock by reducing the forces propagating cracking, which directly translates into an improved service life of the auxiliary material [7-9]. Unfortunately, the glassy phase is also responsible for a dramatic decrease in mechanical properties at high temperatures, which limits the use of mullite panels, cassettes or trays [10]. Under extreme temperature conditions, the phenomenon of creep is very clearly visible [11], which translates into technological problems in high-temperature firing processes at temperatures above 1750°C. Therefore, mullite-based ceramics are widely used for auxiliary materials in the production of ceramic elements whose sintering temperature is lower (approx. 1,400ºC) than in the case of engineering and specialised ceramics, where firing processes are carried out at a temperature of 1700-1800°C [12,13].

Silicon carbide is another material often used for refractory auxiliary panels in the ceramics industry [14-16]. Due to high hardness, excellent corrosion resistance, high thermal stability and wetting resistance of metallic and alkaline slags, silicon carbide (SiC) is widely used in industries requiring heat-resistant materials and/or creep resistance e.g. the lining of blast furnaces [17]. However, SiC-based materials – due to the covalent nature of Si-C bonding and their low self-diffusion rate – cause problems with sintering efficiency in manufacturing processes. Over the past few years, many different binding additives have been tested to overcome this problem. In particular, it has been shown that the addition of oxides promotes the thickening of SiC-based materials by forming a liquid phase during heating, which has an adverse effect on the material operating at high temperatures. The use of different binding phases in SiC ceramics improves the mechanical properties of the finished refractory product but, in most cases, significantly reduces the possible operating temperature. Silicon carbide used for auxiliary elements is characterised by very good operating parameters up to a maximum temperature of 1500°C, above which the material loses its properties and is quickly destroyed. Exposure of the material to such a high temperature in an oxygen atmosphere causes irreversible changes involving the glassy phase on its surface [15-17].

Another material, aluminium oxide, is one of the most important ceramic materials due to the high number of possible applications. Aluminium oxide exists in various metastable structures i.e. so-called transition oxides (such as κ, γ, θ, δ, η) as well as in the stable phase α-Al_2O_3 [18-23]. Of all the oxides listed, potentially the most interesting is α-Al_2O_3 due to its excellent physical and chemical properties, high acid and alkali resistance, high melting point and high hardness. However, as a material for auxiliary elements during firing processes, it is used quite rarely. Aluminium oxide has a high heat capacity, which means that the cooling phase as well as the entire cycle is much longer, which translates into increased production costs. It is also characterised by the highest coefficient of thermal expansion of the materials listed, which does not guarantee constant dimensions of the element and is a very undesirable phenomenon in high-temperature processes [2,24-27].

The subject of the research presented in this study is a new ceramic foundry composite based on a spherical form of aluminium oxide. It is intended to limit the occurrence of technological problems related to the appropriate selection of auxiliary refractory materials through their material properties. The reduced material density, low thermal expansion and lack of reaction with the furnace charge at very high temperatures are to significantly improve the high-temperature firing process. Auxiliary refractory panels made of such a composite can be an alternative to traditionally used materials.

The aim of the research presented in this work was to obtain and characterise a foundry composite based on spherical alumina.

2. Materials and research methods

2.1. Material and preparation of material for research

A composite ceramic material was used in the study, which included the spherical form of aluminium oxide. Two versions of the ceramic material, differing in the percentage share of spherical aluminium oxide in the total volume of the mixture, were made.

In the first material variant, the spherical form of aluminium oxide accounted for 33% of the volume of the entire ceramic mass, while for the second mixture the number of spheres was reduced to 25%.

In both cases, the matrix material was aluminium oxide of a purity of 99.7% (minimum), with a 0.5-2 μm size of raw material grains. However, the binding agents were a polysaccharide and an acrylic binder. The technological recipes of two variants of the ceramic material are presented in Tables 1 and 2.

Table 1.
Shares of individual components of the composite in the first variant

Raw material	Weight, g	Percentage
Aluminium oxide 99.7% – matrix	707.4	33.28%
Aluminium oxide 99.8% – matrix	707.4	33.28%
Aluminium oxide – spheres	707.4	33.28%
Polysaccharide	7.6	0.06%
Acrylic binder	2.3	0.10%

Table 2.
Shares of individual components of the composite in the second variant

Raw material	Weight, g	Percentage
Aluminium oxide 99.7% – matrix	766.4	37.21%
Aluminium oxide 99.8% – matrix	766.4	37.21%
Aluminium oxide – spheres	516.2	25.06%
Polysaccharide	8.3	0.40%
Acrylic binder	2.5	0.12%

The individual components of the mixture were measured out and then mixed with each other using a laboratory agitator to form a thick layer, which was filled with silicone moulds. Samples of the ceramic material were made using gravity casting. The moulded material was predried for a period of 48 hours at room temperature to then move on to drying in a forced warm air dryer at about 40°C for 12 hours. The drying process of the samples was aimed at releasing unbound water. It caused a slight linear shrinkage of the material i.e. 0.7% for Variant 1 and 0.8% for Variant 2.

After the material obtained sufficient rigidity, it could be released from the moulds and subjected to another treatment i.e. high-temperature firing. The firing process was carried out in the Nabertherm HT 276/17/S2 high-temperature electric furnace. The firing process characteristics for both materials are shown in Table 3.

The firing process (Fig. 1), to which the samples were subjected, consisted of an initial phase in which the temperature rose slowly so that the bonding agent contained in the ceramic thickener could be bound. A rapid increase in temperature to the set maximum, in which the material was kept for 5 hours, then followed. Hauschkel and Muche [28] justify the long sintering time by the processes of crystal transformation of the material. During this period, the crystalline remodelling reactions of the material occur and the achieved mechanical and strength properties are determined by this stage.

The next part consists of thickening, during which there are open and irregular pores and the occurring fluxes change into a liquid phase, which clearly affects the shape of the powder particles. The final stage is the growth of the grains of the material by including smaller grains from the boundary areas into their volume [29-31]. The final phase of the high-temperature firing process is the cooling of the furnace, which proceeded slowly up to ambient temperature to avoid stress due to the temperature gradient and possible material degradation.

The samples were subjected to a series of material tests which aimed to confirm its properties as a refractory material that can be used in high-temperature firing processes.

The following tests were carried out as part of the study:

- Structure observations in a scanning electron microscope,
- Water absorption and porosity tests,
- Three-point bending strength tests,
- Measurement of the coefficient of thermal expansion.

Table 3.
Characteristics of the firing process of the tested composite

Segment	Temperature from, Ta, °C	Temperature up to, Tb, °C	Heating rate, K/h	Time, min.
1	40	80	80	30
2	80	80		120
3	80	120	20	120
4	120	120		30
5	120	200	30	160
6	200	200		30
7	200	600	50	480
8	600	1670	80	802
9	1670	1670		300
10	1670	1500	1000	10
11	1500	1500		30
12	1500	1200	100	180
13	1200	1200		15
14	1200	800	50	480
15	800	800		10
16	800	600	100	120
17	600	400	50	240

Maximum temperature	1670 °C
Holding time	5 h
Total time of the process	52.6 h

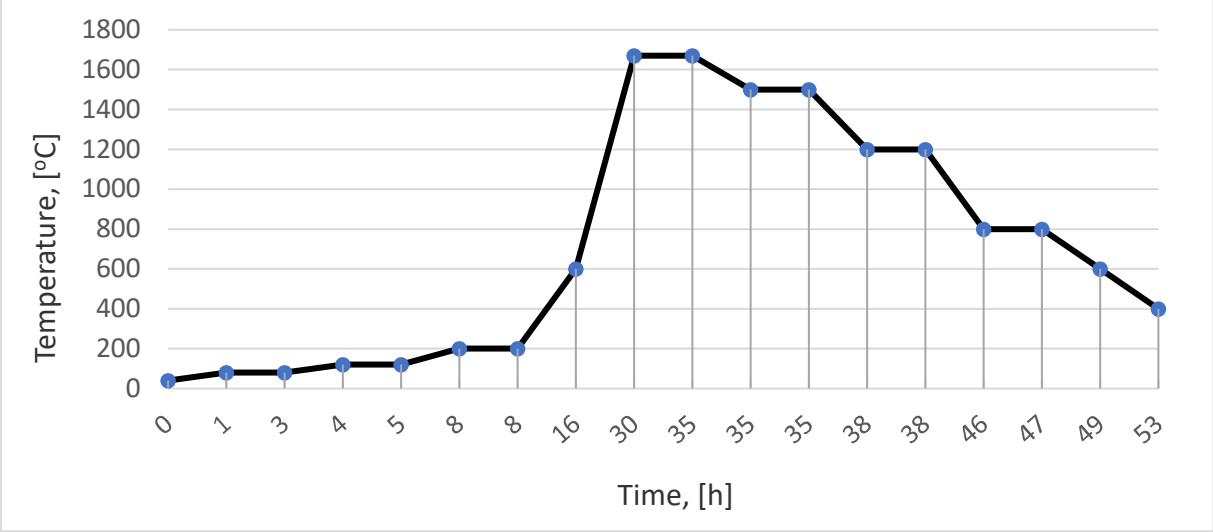

Fig. 1. Graphical presentation of firing process

2.2. Microscopic examination

Structural observations were made on the borders of the samples. A JEOL JSM - 6610LV scanning electron microscope was used for the tests. The observations were made in LV mode. Exemplary images of the structure of the tested samples are shown in Figure 2.

2.3. Water absorption and porosity tests

Water absorption and porosity measurements were made in accordance with PN EN 60672-2:2002 [14]. Samples were cut from a ceramic block and then dried at 120°C. The samples were weighed with an accuracy of 0.01g and then put into a desiccator to which a vacuum pump was connected. After obtaining a pressure inside the device of 3000 Pa, the samples remained in such an arrangement for a period of 30 minutes. Then they were completely covered with demineralised water and left in the desiccator for 3 hours until it was not possible to observe the escape of air bubbles from the inside of the sample material. After this period, the samples were then weighed again. Calculations of porosity and water absorption were made according to the following formulas:

$$P_o = \frac{m_n - m_s}{m_n - m_w} * 100\% \quad (1)$$

where:
P_o – Open porosity, %;
m_{in} – weight of sample measured in water, g;
m_n – weight of a sample saturated with water, g;
m_s – dry sample weight, g.

$$W_A = \frac{m_n - m_s}{m_s} * 100\% \quad (2)$$

where:
W_A – water absorption, %;
m_s – dry sample weight, g;
m_n – mass of the sample saturated with water, g.

The test results are presented in Table 4.

2.4. Bending strength tests of ceramic material

For the three-point bending test, a Zwick Z010 strength machine was used and the tests were carried out in accordance with PN-EN 843-1: 2007.

Sample sets were cut from the ceramic sheet using a circular saw to the dimensions in accordance with the requirements of the standard (Fig. 2).

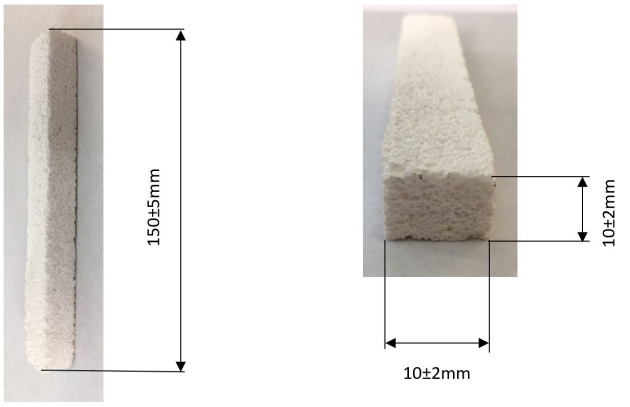

Fig. 2. Samples for strength tests with dimensions in accordance with PN-EN 843-1: 2007 – the measurement results are shown in Table 5

2.5. Thermal expansion coefficient tests

A Netzsch DIL 402C dilatometer was used to test the coefficient of thermal expansion, ensuring a high degree of accuracy, repeatability and temperature stability. This device is characterised by the following measurement parameters:

- temperature range: 20°C-1600°C;
- heating/cooling rate: 0.01 K/min. - 50 K/min.;
- measuring range of the dilatometer: ±500/5000 µm;
- length of samples: max. 50 mm;
- maximum diameter of samples: 12 mm;
- clamping force to the sample from 15-45 cN;

Test specimens measuring 5 mm x 5 mm x 25 mm were cut from a ceramic block using a circular saw. Subsequently, the registration of linear changes of samples in the heating process as a function of temperature was performed.

Heating parameters:

- temperature range in the examination: 20-1500°C;
- heating rate 5deg/min..

Using the registered dilatometric curves, the size of the linear expansion coefficient was calculated using the following formula:

$$\alpha = \frac{\Delta l}{l_0 * \Delta T} \quad (3)$$

where:
Δl – changes in body linear dimensions of length l during heating,
l_0 – initial length of the sample,
ΔT – temperature rise.

Calculations were made for the following temperature ranges 20.6-500°C, 20.6-1000°C, 20.6-1490°C.

3. Test results

3.1. Microscopic examination

Figure 3 presents images of fractures of Variants 1 and 2 obtained using a scanning electron microscope.

Spheres of material in a matrix of pure alumina are visible and there are voids in the cracked grains. The presence of cracks through the spheres indicates good sintering during the firing process. In the event of insufficient sintering, cracks between the spheres would be observed [32-34].

3.2. Water absorption and porosity tests

The Table 4 presents the results of the measurements of water absorption and porosity obtained for both variants of the ceramic material.

The obtained test results correspond to the analysis of images performed in sub-chapter 3.1. It can be observed that for the variant with more spheres, the water absorption and open porosity have a higher value than Variant 2. Cracking of the spheres during sintering creates conditions for capillary fluid absorption during the test, which consequently results in higher values for these quantities.

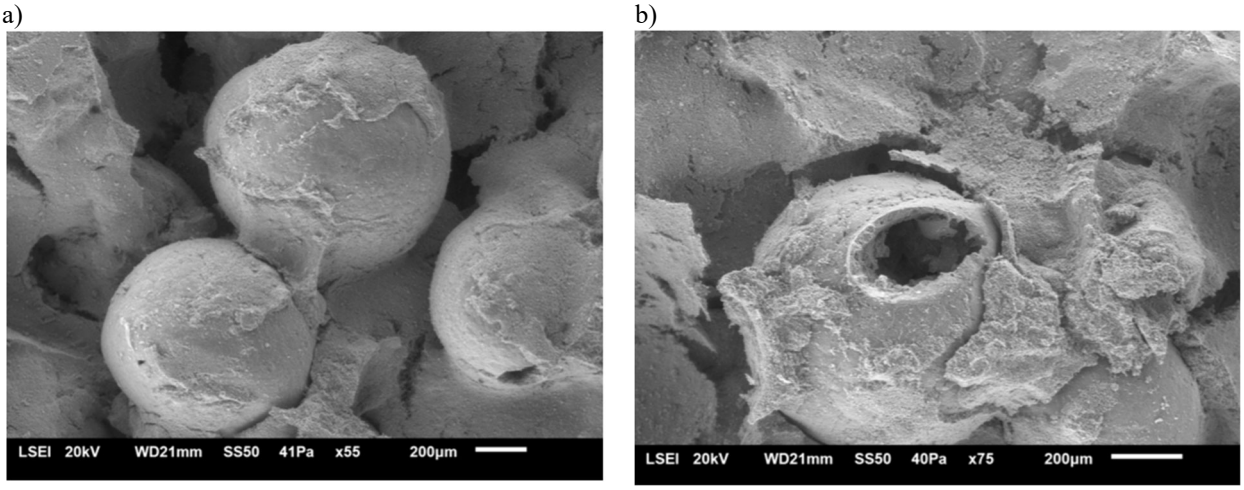

Fig. 3. Surfaces of samples borders: a) sample made according to Variant 1, b) sample made according to Variant 2

Table 4.
Results of measurements of water absorption and porosity of the ceramic material, Variants 1 and 2

Variant of material	Water absorption – average value, %	Water absorption – standard deviation	Open porosity – average value, %	Open porosity – standard deviation
Variant I	26.65	0.79	51.08	0.74
Variant II	22.97	0.10	47.45	0.12

Comparing the obtained results to traditionally used materials, it can be stated that the porosity of the obtained materials is much higher.

The average porosity for mullite is 14-18%, for silicon carbide it is <11%, and for α-Al_2O_3 it is a value in the range of 0-5%[35].

3.3. Bending strength tests of ceramic material

Table 5 shows the obtained bending strength values for both ceramic sample variants.

Table 5.
Results of strength tests for samples of ceramic material Variants 1 and 2

Variant of material	Strength – average value, N/mm^2	Strength – standard deviation
Variant I	6.42	1.71
Variant II	11.42	2.02

Based on the statistics of the data obtained during testing of material samples in Variants 1 and 2, it turned out that

Variant 2 – with a lower content of alumina spheres – showed almost twice as high (11.47 N/mm^2) strength compared to Version 1 (6.88 N/mm^2).

The tests also showed that for the first variant the average deflection value was 0.24-0.4% for 10-14MPa stress. For the second variant, the average deflection value was in the range of 0.25-0.33% at 12-14MPa stress.

3.4. Thermal expansion coefficient tests

Figures 4 and 5 present the obtained dilatometric curves for both ceramic variants, while Tables 6 and 7 show the values of linear expansion coefficients.

At the initial stage, in the low-temperature range, the residual moisture contained in the material evaporates and the organic matter decomposes and burns out. Such phenomena can cause slight shrinkage of the material, which is constantly compensated by an increase in dimensions due to thermal expansion. With a further increase in temperature, a dilatometric curve with a linear relationship between the sample dimensions and the temperature is recorded. Figures 4 and 5 present the results of dilatometric tests of manufactured materials, during which the linear changes of samples in the heating process were recorded as a function of temperature. The Variant 1 sample shows almost linear dependence of dimensional changes as a function of temperature. There is a noticeable period in which the expansion of the material is inhibited, the growth of the dilatometric curve is stopped and the contraction of the system begins. At this point, the material reduces its linear dimensions. Further storage of the material at high temperature shows no further linear changes.

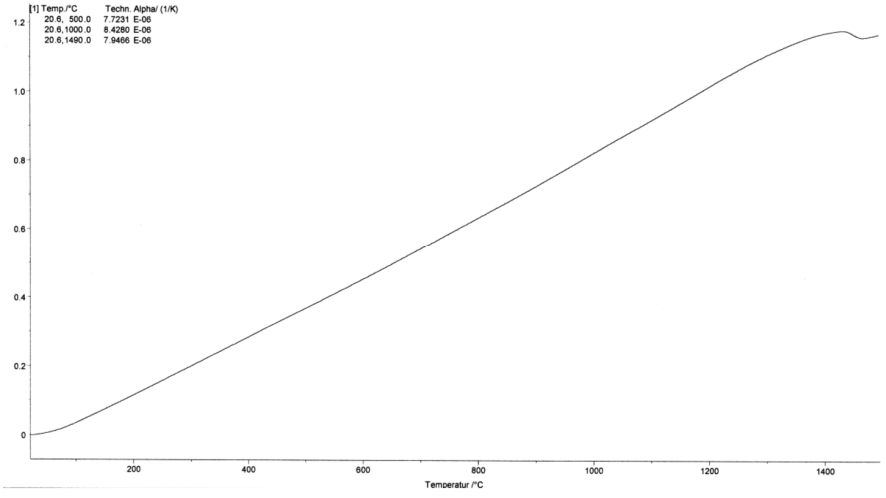

Fig. 4. Diagram of linear changes of material for Variant 1 as a function of temperature

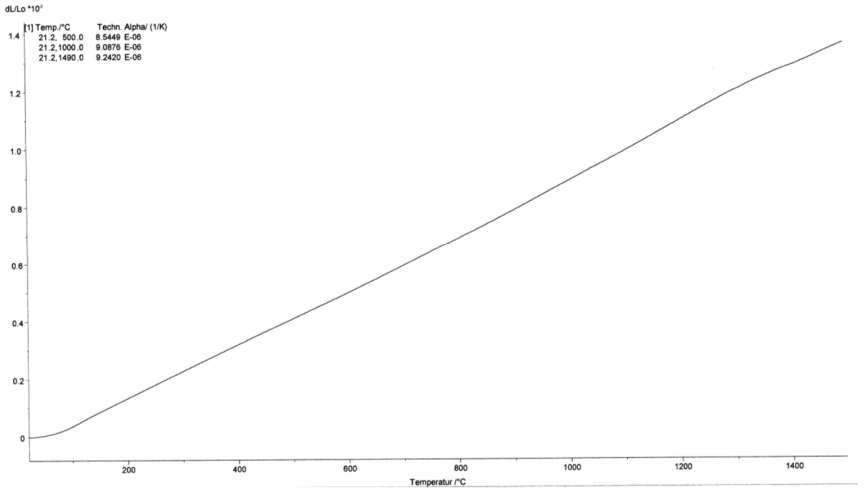

Fig. 5. Diagram of linear changes of material for Variant 1 as a function of temperature

Table 6.
Values of thermal expansion coefficient for Variant 1

Temperature range	Coefficient of thermal expansion, 1/K
20.6-500°C	$7.7231 \cdot 10^{-6}$
20.6-20.6°C	$8.4280 \cdot 10^{-6}$
20.6-1490°C	$7.9466 \cdot 10^{-6}$

Table 7.
Values of thermal expansion coefficient for Variant 2

Temperature range	Coefficient of thermal expansion, 1/K
20.5-500°C	$8.2384 \cdot 10^{-6}$
20.5-1000°C	$8.9443 \cdot 10^{-6}$
20.5-1490°C	$7.6119 \cdot 10^{-6}$

In the case of the material according to Variant 2, the initial period of moisture evaporation or burning of organic materials at low temperatures, of up to 100°C, is more visible. This is due to the increased volume of the matrix, which means that a more compact material needs more time to dry or burn some components of the ceramic material. After this period, as in the material according to Variant 1, a linear increase in the dimensional changes of the samples depending on the temperature is observed up to a temperature of about 1400°C.

The differences at higher temperatures between the graphs of heating rate as a function of temperature for two material variants (Figs. 4 and 5) may be associated with transformations of the crystallographic structure of the material together with temperature changes. This is due to the fact that all alumina polymorphs are converted to α-Al_2O_3 after calcination at 800-1200°C. The last step in the thermal transformation of alumina is usually a phase transition from θ-Al_2O_3 to α-Al_2O_3, which occurs suddenly in a narrow temperature range, as indicated by a well-defined endothermic (during heating) DTA signal between 1200 and 1400°C [36]. This transition is accompanied by a loss of porosity and surface area, as well as some increase in crystal size. Therefore, the signal in the graphs is associated with the change in the crystal structure of alumina from θ to α. In chart 4 the area of endothermic transformation for material of variant 1 is more pronounced, which is related to the number of spheres used to prepare the samples.

4. Analysis of results and conclusions

The study showed that the quantitative share of the spherical form of Al_2O_3 in the volume of ceramic material has a major impact on its properties. An increased share of spheres translates into greater material porosity and lower matrix density but also, unfortunately, by reducing the cross-section, into decreased strength properties. Literature data on the strength of ceramic materials shows that the new material based on spherical alumina does not have such high properties as mullite materials or silicon carbide. The strength of mullite materials reaches 200 MPa, for SiC it is 300 MPa, while for alumina ceramics this value increases to 500 MPa [16,28] which, compared to the composite material with alumina spheres [6.88 MPa (Variant 1) and 11.47 MPa (Variant 2)], is currently not achievable and constitutes a further direction of research and development of the material. However, considering the planned use of the material – as the refractory panel does not carry too many mechanical loads – the achieved strength parameters may be sufficient.

Comparing the obtained results to traditionally used materials, it can be stated that the porosity of the obtained materials is much higher.The average porosity for mullite is 14-18%, for silicon carbide it is <11%, and for α-Al_2O_3 it is a value in the range of 0-5%.

The table values of the coefficient of thermal expansion for alumina are in the range of 6 to $9 \cdot 10^{-6}$ 1/K, depending on the form of the material and the results obtained are in line with literature reports [35]. The results of tests of thermal expansion of samples for Variants 1 and 2 showed that for Variant 1 the coefficient of thermal expansion varies in the range of 7.7 to $8.7 \cdot 10^{-6}$ 1/K and, in the case of material according to Variant 2, is slightly higher and is within the range of $7.6\text{-}9.2 \cdot 10^{-6}$ 1/K. According to the source literature [16,28], the coefficient of thermal expansion for alumina ceramics without holospheres at 20°C is $26 \cdot 10^{-6}$ 1/K and, at 1400°C, amounts only to $4 \cdot 10^{-6}$ 1/K. For mullite materials, the difference is not as high and the value of the coefficient varies from $6 \cdot 10^{-6}$ 1/K (20°C) up to $3 \cdot 10^{-6}$ 1/K (1400°C). For ceramics based on silicon carbide, this value is almost constant in the temperature range 20-1400°C and amounts to $4.8 \cdot 10^{-6}$ 1/K. In the case of the developed ceramic material, there is no visible trend of a decrease in the coefficient of thermal expansion with increasing temperature, which is the case with traditional ceramic materials. It seems that reducing the coefficient of thermal expansion may be beneficial because, as a result, it will reduce potential stresses in the panels and thus the risk of damage.

Bibliography

[1] D.J. Duval, S.H. Risbud, J.F. Shackelford, Mullite, in: J.F. Shackelford, R.H. Doremus (Eds.), Ceramic and Glass Materials: Structure, Properties and Processing, Springer, Boston, 2008, 27-39, DOI: https://doi.org/10.1007/978-0-387-73362-3_2.

[2] H. Schneider, J. Schreuer, B. Hildmann, Structure and properties of mullite-A review, Journal of the European Ceramic Society 28/2 (2008) 329-344, DOI: https://doi.org/10.1016/j.jeurceramsoc.2007.03.017.
[3] J. Anggono, Mullite Ceramics: Its Properties Structure and Synthesis, Jurnal Teknik Mesin Universitas Kristen Petra 7/1 (2005) 1-10, DOI: https://doi.org/10.9744/jtm.7.1.pp.1-10.
[4] H. Schneider, R.X. Fischer, J. Schreuer, Mullite: Crystal Structure and Related Properties, Journal of the American Ceramic Society 98/10 (2015) 2948-2967, DOI: https://doi.org/10.1111/jace.13817.
[5] M.I. Osendi, C. Baudín, Mechanical Properties of Mullite Materials, Journal of the European Ceramic Society 16/2 (1996) 217-224, DOI: https://doi.org/10.1016/0955-2219(95)00133-6.
[6] H. Schneider, M. Schmüker, K.J.D. Mackenzie, Basic Properties of Mullite, in: H. Schneider, S. Komarneni (Eds.), Mullite, Wiley, 2006, 141-225, DOI: https://doi.org/10.1002/3527607358.ch2.
[7] L. Carbajal, F. Rubio-Marcos, M.A. Bengochea, J.F. Fernandez, Properties related phase evolution in porcelain ceramics, Journal of the European Ceramic Society 27/13-15 (2007) 4065-4069, DOI: https://doi.org/10.1016/j.jeurceramsoc.2007.02.096.
[8] F.J. Torres, E. Ruiz de Sola, J. Alarcón, Mechanism of crystallization of fast fired mullite-based glass-ceramic glazes for floor-tiles, Journal of Non-Crystalline Solids 352/21-22 (2006) 2159-2165, DOI: https://doi.org/10.1016/j.jnoncrysol.2006.01.038.
[9] F. Chargui, M. Hamidouche, H. Belhouchet, Y. Jorand, R. Doufnoune, G. Fantozzi, Mullite fabrication from natural kaolin and aluminium slag, Boletín de la Sociedad Española de Cerámica y Vidrio 57/4 (2018) 169-177, DOI: https://doi.org/10.1016/j.bsecv.2018.01.001.
[10] F. Nadachowski, Outline of refractory technology, Silesian Technical Publishers, Katowice, 1995 (in Polish).
[11] G. Routschka, L.M. Hamersley, J. Hamersley, Pocket manual refractory materials: Basics, structures, properties, Vulkan-Verlag, Essen, 2004.
[12] F.J. Klug, S. Prochazka, R.H. Doremus, Alumina-Silica Phase Diagram in the Mollite Region, Journal of the American Ceramic Society 70/10 (1987) 750-759, DOI: https://doi.org/10.1111/j.1151-2916.1987.tb04875.x.
[13] N.L. Bowen, J.W. Greig, The system: Al_2O_3.SiO_2. Journal of the American Ceramic Society 7/4 (1924) 238-254, DOI: https://doi.org/10.1111/j.1151-2916.1924.tb18190.x.
[14] R.B. Sosman, A pilgrimage to Mull, American Ceramic Society Bulletin 35/3 (1956) 52-54.
[15] J.-H. Eom, Y.-W. Kim, S. Raju, Processing and properties of macroporous silicon carbide ceramics: A review, Journal of Asian Ceramic Societies 1/3 (2013) 220-242, DOI: https://doi.org/10.1016/j.jascer.2013.07.003.
[16] G.W. Meetham (Chief), Engineering ceramics: Part E of 'Requirements for and factors affecting high temperature capability', Materials and Design 10/3 (1989) 138-143, DOI: https://doi.org/10.1016/s0261-3069(89)80029-9.
[17] J. Kriegesmann, Processing of silicon carbide-based ceramics, Comprehensive Hard Materials 2 (2014) 89-175, DOI: https://doi.org/10.1016/B978-0-08-096527-7.00023-4.
[18] S.-K. Lee, M. Tatsumisago, T. Minami, The Ceramic Society of Japan NII-Electronic Library Service, Journal of the Ceramic Society of Japan, 1997.
[19] P. De Silva, K. Sagoe-Crenstil, V. Sirivivatnanon, Kinetics of geopolymerization: Role of Al_2O_3 and SiO_2, Cement and Concrete Research 37/4 (2007) 512-518, DOI: https://doi.org/10.1016/j.cemconres.2007.01.003.
[20] S. Cava, S.M. Tebcherani, I.A. Souza, S.A. Pianaro, C.A. Paskocimas, E. Longo, J.A. Varela, Structural characterization of phase transition of Al_2O_3 nano-powders obtained by polymeric precursor method, Materials Chemistry and Physics 103/2-3 (2007) 394-399, DOI: https://doi.org/10.1016/j.matchemphys.2007. 02.046.
[21] A. Boumaza, L. Favaro, J. Lédion, G. Sattonnay, J.B. Brubach, P. Berthet, A.M. Huntz, P. Roy, R. Tétot, Transition alumina phases induced by heat treatment of boehmite: An X-ray diffraction and infrared spectroscopy study, Journal of Solid State Chemistry 182/5 (2009) 1171-1176, DOI: https://doi.org/10.1016/j.jssc.2009.02.006.
[22] R. McPherson, Formation of metastable phases in flame- and plasma-prepared alumina, Journal of Materials Science 8 (1973) 851-858, DOI: https://doi.org/10.1007/BF02397914.
[23] K.M. Shorowordi, T. Laoui, A.S.M.A. Haseeb, J.P. Celis, L. Froyen, Microstructure and interface characteristics of B_4C, SiC and Al_2O_3 reinforced Al matrix composites: A comparative study, Journal of Materials Processing Technology 142/3 (2003) 738-743, DOI: https://doi.org/10.1016/S0924-0136(03)00815-X.
[24] P. Auerkari, Mechanical and physical properties of engineering alumina ceramics, VTT Tied - Valt Tek, Tutkimusk, 1996.
[25] P.J. Karditsas, M.-J. Baptiste, Aluminium oxide, in: Thermal and Structural Properties of Fusion Related

Materials, Avaliable from: http://www-ferp.ucsd.edu/LIB/PROPS/PANOS/al2o3.html.
[26] B.J. Ash, D.F. Rogers, C.J. Wiegand, L.S. Schadler, R.W. Siegel, B.C. Benicewicz, T. Apple, Mechanical properties of Al_2O_3/polymethylmethacrylate nanocomposites, Polymer Composites 23/6 (2002) 1014-1025, DOI: https://doi.org/10.1002/pc.10497.
[27] H.J. Wang, Z.H. Jin, Y. Miyamoto, Effect of Al_2O_3 on mechanical properties of Ti_3SiC_2/Al_2O_3 composite, Ceramics International 28/8 (2002) 931-934, DOI: https://doi.org/10.1016/S0272-8842(02)00076-7.
[28] H. Heuschkel, G. Heuschkel, K. Muche, ABC Keramik: mit 77 Tabellen und einem Kunstdruckteil, Dt. Verlag für Grundstoffindustrie, 1990 (in German).
[29] Z. Károly, J. Szépvölgyi, Hollow alumina microspheres prepared by RF thermal plasma, Powder Technology 132/2-3 (2003) 211-215, DOI: https://doi.org/10.1016/S0032-5910(03)00077-9.
[30] W. Lee, S. Choi, S.M. Oh, D.W. Park, Preparation of spherical hollow alumina particles by thermal plasma, Thin Solid Films 529 (2013) 394-397, DOI: https://doi.org/10.1016/j.tsf.2012.05.048.
[31] N.V. Kulkarni, S. Karmakar, S.N. Asthana, A.B. Nawale, A. Sheikh, S.P. Patole, J.B. Yoo,V.L. Mathe, A.K. Das, S.V. Bhoraskar, Study on growth of hollow nanoparticles of alumina, Journal of Materials Science 46 (2011) 2212-2220, DOI: https://doi.org/10.1007/s10853-010-5059-2.
[32] Z. Su, X. Xi, Y. Hu, Q. Fei, S. Yu, H. Li, J. Yang, A new Al_2O_3 porous ceramic prepared by addition of hollow spheres, Journal of Porous Materials 21 (2014) 601-609, DOI: https://doi.org/10.1007/s10934-014-9806-7.
[33] J.A. Santa Maria, B.F. Schultz, J.B. Ferguson, P.K. Rohatgi, Al-Al_2O_3 syntactic foams – Part I: Effect of matrix strength and hollow sphere size on the quasi-static properties of Al-A206/Al_2O_3 syntactic foams, Materials Science and Engineering: A 582 (2013) 415-422, DOI: https://doi.org/10.1016/j.msea.2013.05.081.
[34] J.A. Santa Maria, B.F. Schultz, J.B. Ferguson, N. Gupta, P.K. Rohatgi, Effect of hollow sphere size and size distribution on the quasi-static and high strain rate compressive properties of Al-A380-Al_2O_3 syntactic foams, Journal of Materials Science 49 (2014) 1267-1278, DOI: https://doi.org/10.1007/s10853-013-7810-y.
[35] R. Pampuch, Modern ceramic materials, AGH Publishing House, Cracow, 2005 (in Polish).
[36] R.W. Grimshaw, A.B. Searle, The chemistry and physics of clays and allied ceramic materials, 1971.